Atmospheric new particle formation as source of CCN in the Eastern Mediterranean marine boundary layer

N. Kalivitis[1,2], V.-M. Kerminen[2], G. Kouvarakis[1], I. Stavroulas[1], A. Bougiatioti[3,8], A. Nenes[3,5,6], H.E. Manninen[2,4], T. Petäjä[2], M. Kulmala[2] and N. Mihalopoulos[1,7,9]

1. Environmental Chemical Processes Laboratory, Department of Chemistry, University of Crete, 71003, Heraklion, Greece

2. Department of Physics, University of Helsinki, P.O. Box 64, FI-00014, University of Helsinki, Finland

3. School of Earth and Atmospheric Sciences, Georgia Institute of Technology, Atlanta, GA 30332,USA

4. Institute of Physics, University of Tartu, Ülikooli 18, 50090, Tartu, Estonia

5.School of Chemical & Biomolecular Engineering, Georgia Institute of Technology, Atlanta, GA, 30332,USA

6. ICE-HT, Foundation for Research and Technology, Hellas, 26504, Patras, Greece

7. Institute for Environmental Research & Sustainable Development, National Observatory of Athens (NOA), I. Metaxa & Vas. Pavlou, 15236 Palea Penteli, Greece

8. National Technical University of Athens, Zografou Campus, 15780, Athens, Greece

9. Energy, Environment and Water Research Center, The Cyprus Institute, Nicosia 2121, Cyprus

Abstract

While Cloud Condensation Nuclei (CCN) production associated with atmospheric new particle formation (NPF) is thought to be frequent throughout the continental boundary layers, few studies on this phenomenon in marine air exist. Here, based on simultaneous measurement of particle number size distributions, CCN properties and aerosol chemical composition, we present the first direct evidence on CCN production resulting from NPF in the Eastern Mediterranean atmosphere. We show that condensation of both gaseous sulfuric acid and organic compounds from multiple sources leads to the rapid growth of nucleated particles to CCN sizes in this environment during the summertime. Sub-100 nm particles were found to be substantially less hygroscopic than larger particles during the period with active NPF and growth (the value of κ was lower by 0.2–0.4 for 60 nm particles compared with 120 nm particles), probably due to enrichment of organic material in the sub-100nm size range. The aerosol hygroscopicity tended to be at minimum just before the noon and at maximum in afternoon, which was very likely due to the higher sulfate to organic ratios and higher degree of oxidation of the organic material during the afternoon. Simultaneously to the formation of new particles during daytime, particles formed in the previous day or even earlier were growing into the size range relevant to cloud droplet activation, and the particles formed in the atmosphere were possibly mixed with long-range transported particles.

1. Introduction

Aerosol particles influence the Earth's radiation balance via aerosol-radiation and aerosol-cloud interactions, the latter effect constituting one of the largest uncertainties in understanding the anthropogenic climate change (IPCC, 2013). A key quantity related to aerosol-cloud interactions is the number concentration of aerosol particles able to act as cloud condensation nuclei (CCN) at water vapour supersaturation levels relevant for ambient clouds. Supersaturations in the atmospheric water clouds remain well below 10% and most frequently below 1% (Pruppacher and Klett, 1997). The probability by which an aerosol particle acts as a CCN at a given supersaturation depends primarily on its size and secondarily on its chemical composition (Dusek et al., 2006). In a population of aerosol particles, the total CCN number concentration is affected by the chemical composition and mixing state of these particles (Karydis et al., 2012; Padró et al., 2012).

CCN are emitted directly to the atmosphere by a variety of natural and anthropogenic sources, in addition to which CCN can also be produced in the atmosphere by the growth of both primary and secondary aerosol particles (Andreae and Rosenfeld, 2008; Pierce and Adams, 2009). Model studies suggest that a large fraction of CCN in the global atmosphere originates from atmospheric new particle formation (NPF) and growth. Merikanto et al., (2009) estimated that 45% of the global low-level-cloud CCN at 0.2% supersaturation result from nucleation (ranging between 31–49%). Westervelt et al., (2014) estimated the average global increase of the boundary-layer CCN number concentration at 0.2% supersaturation due to nucleation ranging between 49 % and 78%, depending on the simulation scenario used. The fraction of nucleated particles that can grow to CCN sizes in the boundary layer is likely to have large spatial variations, ranging from <20% for 0.4% supersaturation for Southern Ocean and exceeding 60% for the tropical oceans, Antarctica, Eastern United States, Europe and North Atlantic, whereas in the vertical dimension CCN concentration generally decrease with an increasing altitude (Yu and Luo, 2009). Field studies directly investigating the connection between atmospheric NPF, subsequent particle growth and CCN production have been mostly limited to continental boundary-layer sites (see Kerminen et al., 2012, and references therein). An example of increase in CCN sized particles concentration after coastal nucleation is presented in O. Dowd, 2001 In general, however, field measurements give support for the potentially important role of NPF in CCN production, at least regionally; nucleation observed was followed by increase in CCN number concentrations.

New particle formation is frequent in the Eastern Mediterranean atmosphere (Petäjä et al. 2007, Kalivitis et al., 2008, Manninen et al., 2010, Kalivitis et al., 2012, Pikridas at al., 2012), although a bit more sparse than in other, mostly continental, European sites (Manninen et al., 2010). Few CCN measurements have been conducted in the Eastern Mediterranean (Bougiatioti et al., 2009, 2011), and no attempt exist to date to link NPF with CCN in this environment. This study will focus on the NPF-CCN link using observations of particle number size distribution, CCN and high resolution aerosol chemical composition. The specific scientific questions, we aim to address are the following: 1) does atmospheric NPF lead to the production of new CCN in the Eastern Mediterranean atmosphere, 2) what is the relative role of sulfuric acid and low-volatile organic vapors of different origin in growing nucleated particles to CCN sizes, 3) how does the hygroscopicity of particles relevant to the cloud droplet activation vary with the particle size and time of day, and 4) what implications our findings will have on quantifying the main sources of CCN in this environment.

2. Materials and methods

2.1 Measurements location

Measurements were performed between 20 August and 25 November 2012 at the atmospheric observation station of the University of Crete at Finokalia, Crete, Greece (35˚20΄N, 25˚40΄E, 250m a.s.l). The Finokalia station (http://finokalia.chemistry.uoc.gr/) is a European supersite for aerosol research, part of the ACTRIS (Aerosols, Clouds, and Trace gases Research Infrastructure) Network. The station is situated directly at the top of a hill over the coastline, in the north east part of the island of Crete, facing the Mediterranean Sea in the wide north sector. Air masses sampled at Finokalia represent the marine conditions of Eastern Mediterranean (Lelieveld et al., 2002), only very slightly influenced by local anthropogenic sources. The nearest major urban center in the area is Heraklion with approximately 170 000 inhabitants, located about 50 km to the west of the measurement site. A detailed description of the Finokalia station and the climatology of the area can be found in Mihalopoulos et al. (1997).

2.2 Instrumentation

The particle number size distributions were measured in the diameter range 9−848 nm using a custom-built Scanning Mobility Particle Sizer (SMPS). The system is closed-loop, with a 5:1 ratio between the aerosol and sheath flow, it consists of a Kr-85 aerosol neutralizer (TSI 3077), a Hauke medium Differential Mobility Analyzer (DMA) and a TSI-3772 Condensation Particle Counter (CPC), and it is operated following the recommendations by Wiedensohler et al.(2012). The sampling was made through a PM_{10} sampling head and the sample humidity was regulated below the relative humidity of 40% with the use of Nafion® dryers in both the aerosol and sheath flow. The measured number size distributions were corrected for diffusional particle losses.

The chemical composition of the non-refractive mass of submicron particles was specified with an Aerodyne Research Aerosol Chemical Speciation Monitor (ACSM ; Ng et al., 2011). The ACSM provides real-time (30-min time interval) information on ammonium, sulfate, nitrate, chloride and organic mass in non-refractory submicron particles. More details and calculations of the mass concentrations can be found in Bougiatioti et al. (2014). During our measurements, the ambient air was drawn into the ACSM via a PM_1 aerosol inlet without sample drying. The concentration of black carbon (BC) was measured using an AE31 Aethalometer (Magee Scientific, AE31) operated with a PM_{10} sampling head and under humidity controlled conditions.

Aethalometer data were corrected using the empirical formula given by Weingartner et al. (2003). In this formula (their equation 4), the calibration constant *C* has been calculated to be 2.48 for the Finokalia station in summer and *R*(ATN) was taken as 1, the value representative for aged particles at remote locations (Sciare et al., 2008).

In order to investigate size-segregated CCN properties, we utilized a coupled DMA-CCNc set-up. The sampled polydisperse aerosol were driven through a TSI 3080 DMA after being charged by a Kr-85 aerosol neutralizer (TSI 3077). The DMA had a closed-loop system for recirculating the sheath flow. The monodisperse aerosol, classified at the 60, 80, 100 and 120 nm diameters out of the DMA, were then supplied to a Continuous Flow Streamwise Thermal Gradient CCN Chamber (CFSTGC; Roberts and Nenes, 2005) in order to determine the number concentration of aerosol particle able to act as CCN with respect to supersaturation. The CFSTGC was operated in the "Scanning Flow CCN Analysis" (SFCA) mode (Moore and Nenes, 2009), in which the flow rate in the CCN instrument is ranged over 1-2 minute cycles while maintaining the temperature gradient constant, which allows supersaturation to change during a flow cycle and results in a CCN spectrum every 1-2 minutes. In this study, the flow rate was varied linearly between 300 and 1000 cm^{-3} min^{-1}. Calibrations by using laboratory-generated ammonium sulfate particles of different sizes, following the procedure of Moore and Nenes (2009), were performed once every month, to verify the stability of the system. The calibration curves relating the supersaturation to the flow rate were calculated based on Köhler Theory. The absolute uncertainty of the calibrated CCNc supersaturation has been estimated to be ±0.04% (Moore et al., 2012). The total number concentration of particles (CN) was measured after the DMA. During the periods when the DMA was inoperative, the CCNc was operated at the total CCN mode where the CCN number concentration was monitored at a fixed supersaturation of 0.2%, using similar settings to Bougiatioti et al., (2009). During the study period concentrated in this paper (28 August to 2 September 2012), size-segregated CCN measurements were not available after 22:55 on 30 August, and the total CCN concentration measurements at the 0.2% supersaturation initiated at 23:15 on 1 September.

2.3 Data analysis

The CCN activation potential of the classified aerosol can be characterized with the help of the Activation Fraction (AF) defined as the CCN/CN ratio. By plotting the AF as a function of flow rate of CCNc, and thus as a function of supersaturation, the result can be fitted to a sigmoidal curve (Bougiatioti et al., 2011), where the maximum AF at the highest supersaturation measured

is the asymptote of the curve. An example of a sigmoid activation curve is shown in Fig. 1. The flow rate Q_{50} describes the inflection point of the sigmoidal curve and corresponds to the critical supersaturation, S_c, above which particles act as CCN (Moore and Nenes, 2009). Once the value of S_c has been obtained, the hygroscopic parameter kappa (κ), can be calculated from Köhler theory using the single parameter approach of Petters and Kreidenweis (2007):

$$\kappa = \frac{4A^3}{27 D_d^3 s_c^2}, A = \frac{4 M_w \sigma_w}{RT\rho_w},$$

where M_w is the molar mass of water, σ_w is the surface tension of water, R is the universal gas constant, T is temperature, ρ_w is the density of water and D_d is the particle dry diameter. The value of κ is 0 for non-hygroscopic material and lies typically in the range 0.01−0.5 for slightly-to-highly hygroscopic organic compounds and in the range 0.5−1.5 for hygroscopic inorganic compounds (Petters and Kreidenweis, 2007).

We divided the organic mass measured with the ACSM into a few separate components using the positive matrix factorization (PMF) analysis (Paatero, 1999). For this purpose, we utilized the multi-linear solver ME-2 using the interface described by Canonaco et al. (2013). The estimated oxygen-to-carbon ratios (O/C) of the organic material were calculated following the approach by Aiken et al. (2008). Atomic O/C ratios characterize the oxidation state of organic aerosol which correlates to their density and water solubility. It has been shown that κ generally increases with the organic oxidation level (eg. Massoli et al., 2010; Mei et al., 2013), however it should be noticed that several other studies have shown that the link between hygroscopicity and oxidation level is not straightforward (Cerully et al. 2014 and references therein)

We determined the particle growth rate (GR) during the new-particle formation events along with the condensation sink (CS), using the approach described in detail by Kulmala et al. (2012). The values of GR discussed later in this paper refer to the particle growth rates of 9−20 nm diameter particles averaged over each NPF event.

3. Results

We chose 28 August to 2 September, 2012 as our case study period, since during that time several NPF events were observed at the Finokalia station as shown in the size distributions in Fig. 2. For three consecutive days (29−31 August), NPF formation was observed before noon at the lowest detectable sizes, with subsequent growth of the newly-formed particles over the rest of the day

(Fig. 2). These days are typical examples of so-called regional NPF events, in which the particle formation and growth takes almost homogeneously place over distances of tens to hundreds of kilometers (Kulmala et al., 2012). During this time period, a low pressure system moved over the north of the Balkan Peninsula heading eastwards, and as a result the air mass origin shifted from W/NW to N/NE from the island of Crete. Four-day air mass back-trajectories calculated using the HYSPLIT model (Draxler and Hess, 1998) showed that the air masses leading to NPF during these three days originated from the free troposphere and then descended to the marine boundary layer approximately 5, 9 and 12 hours, respectively, prior to the initiation of the events (Fig. 3). A decline of air from higher altitudes into the marine boundary layer prior to NPF at Finokalia has been reported in the past as well (Kalivitis et al., 2012). It is worth noting that the back trajectories during the previous days did not show such an air mass descend. Satellite images showed broken to overcast cloud conditions over Black Sea on 28 August, quickly evaporating the following day. No significant change in the origin of the air masses during the three events on 29−31 September was observed, so in the following analysis our main focus will be on these three days.

The first (28 August) and fifth (1 September) of the events showed clear signs of the particle growth up to several tens of nm, but the newly-formed particles were not observed until they had already reached sizes larger than 20−30 nm. During these two days, NPF apparently did not take place in the immediate vicinity of the station but had rather been initiated at least a few hours before the air masses entered our measurement site. During the night between 1 and 2 September, a NPF event was observed with no apparent growth of the particles beyond the nucleation mode. Nighttime NPF events with very limited growth are relatively common in Finokalia, and such events tend to be associated with air mass transport over the island of Crete (Kalivitis et al., 2012). These features point toward the local origin of such events, so in the following analysis we will not consider the nighttime event any further.

3.1 Aerosol growth and CCN production

A key quantity in estimating the CCN production associated with atmospheric nucleation is the particle growth rate, GR, since it determines the time lag between nucleation and subsequent CCN production, and affects the fraction of nucleated particles that eventually reach CCN sizes before being lost by coagulation scavenging or other removal processes (e.g. Kerminen et al.,

2012; Westervelt et al., 2014). The observed values of GR on 29, 30 and 31 August were 3.3, 1.8 and 3.6 nm h^{-1}, respectively, which are lower than the annually-averaged (±STD) GR of 5.2 ±3.4 nm h^{-1} reported by Pikridas et al.(2012) at the same site for the 10-25 nm size range. By following the approach of Laakso et al. (2013), we could follow the growth of newly-formed particles up to about 50−60 nm in particle diameter until another NPF occurred or the particle growth was interrupted by an air mass or cloud cover change. These features are suggestive of the convolution of nucleation with condensational growth of both new and preexisting particles formed in the previous day (or even earlier) to produce CCN size range particles.

When no CCN measurements are available, a commonly-used proxy for the CCN number concentration is the total number concentration of particles larger than some threshold diameter, *D*, denoted as N_D (Paasonen et al., 2013, Laakso et al., 2013). Just prior to the nucleation event period (28 August − 2 September) and after it, our CCN counter was offline the DMA due to technical problems, so that it was recording the total CCN number concentration at 0.2% supersaturation, $CCN_{0.2}$. The measured values of $CCN_{0.2}$ correlated strongly with N_{90}, N_{100}, N_{110}, N_{120} and N_{130} (Fig. 4) when considering all the available data. The relation between $CCN_{0.2}$ and N_D prior to the three-day period with most active new particle formation and growth differed greatly from the corresponding relation after this period. Prior to the NPF events (Fig. 4a), the best correlation against $CCN_{0.2}$ was observed for N_{90}, but this quantity overestimated heavily the CCN concentration (R^2=0.95, slope = 1.73). With increasing diameters, D, the value of R^2 decreased as did also the slope, so that between N_{130} and $CCN_{0.2}$ the weakest correlation and smaller slope was observed (R^2=0.78, slope = 1.17). On the other hand, after the NPF events (Fig. 4b) the picture was different: for N_{90} the correlation with $CCN_{0.2}$ was still very good (R^2=0.94, slope = 1.43), for diameters larger than 110 nm this slope dropped below 0.45, and for particles larger than 120 or 130 nm there was practically no correlation between N and $CCN_{0.2}$. The slope of the above regression analysis probably reflects the activation fraction for each diameter while R^2 values indicate that, especially in active NPF periods, the variability of CCN number may be controlled by sub-100 nm particle population. Overall, these data suggest that during active NPF periods, particles larger than about 100 nm in diameter were able to act effectively as CCN at 0.2% supersaturation in the measured air masses, which is in line with observations made elsewhere (see Kerminen et al., 2012); we therefore recommend N_{100} as a proxy for $CCN_{0.2}$ at Finokalia with a linear correction in a form $CCN_{0.2}=a*N_{100}+b$, where a and b are the slope and offset determined from our observations. For the dataset considered here, a= 0.57 ± 0.01 and b =

180 ± 9 cm−3, where ± represents the standard error with respect to the linear fit for all the data in Fig. 4.

Next, we will examine the time evolution of the CCN proxies during our case study period (Fig. 5). We may see that the increase in the total particle number concentration, N_{tot}, caused by nucleation was often followed by an increase in N_{50} after some time lag, as one would expect due to the gradual growth of newly-formed particles up to 50 nm during the same day. The time evolution of both N_{100} and N_{130} resembled that of N_{50}, but with the difference that the base levels of N_{100} and N_{130} tended to increase gradually over time after 29 August. This latter feature supports our earlier speculation that CCN production was a multi-day process in measured air masses, at least when it comes to the CCN that are active at low supersaturations between about 0.1 and 0.3%. It should be noted that the origin of the new CCN was not necessarily only atmospheric nucleation, but also the growth of sub-CCN-size primary particles during their transportation. The apparent co-variation of N_{50}, N_{100} and N_{130} reveals that, besides new-particle formation and growth, the measured air masses had been affected to variable extents by i) dilution due to the free-troposphere entrainment, and ii) long-range-transported primary aerosol particles.

3.2 Aerosol chemical composition, hygroscopicity and CCN activity

To obtain a comprehensive understanding on particle CCN activity properties, we quantified the link between aerosol chemical composition and hygroscopicity. Fig. 6 shows that the composition of submicron particulate matter was dominated by organic material (average concentration 1.9±0.9 μg m^{-3}) and sulfate including associated ammonium (1.8±0.8 μg m^{-3}) during our case study period, while nitrate and black carbon contributed a minor fraction of the aerosol (average concentration 0.13±0.08 and 0.34±0.15 μg m^{-3} respectively). Long-term measurements at Finokalia are in line with this pattern (eg Lelieveld et al., 2002; Bougiatioti et al., 2013), suggesting that the relative abundances of sulfate and organic matter dictate to large extent the hygroscopic and cloud activating properties of submicron particles at Finokalia.

In a broader picture, when averaged for the period 1 August to 30 September, the aerosol chemical composition displayed a clear diurnal pattern (Fig. 7a). In general, sulfate concentrations started to increase very rapidly around the noon and reached their diurnal maximum during afternoon, after which they decreased first gradually and then more rapidly until the following noon. The afternoon increase in the sulphate concentration can be ascribed to the intensive photochemical production of gaseous sulphuric acid from both natural and

anthropogenic precursors during daytime, followed by the condensation of sulphuric acid into pre-existing aerosol particles together with gaseous ammonia (e.g. Zerefos et al., 2000; Kouvarakis and Mihalopoulos, 2002; Bardouki et al., 2003; Mihalopoulos et al., 2007). Since sulphate is practically non-volatile, the decreasing sulphate concentrations during night and morning hours are most likely a combination of air mass dilution by entrainment and aerosol deposition processes. Organic material declined less rapidly than sulfate during morning, suggesting that secondary organic aerosol (SOA) formation was very active already before noon or, alternatively, that the organic material was less sensitive to dilution than sulfate, i.e. the concentration gradient between the mixed layer and air above it was smaller for organic material than sulphate. After noon, organic material did not increase as rapidly as sulfate, which might be either due to different photochemical pathways for sulphate and SOA formation (see e.g., Ehn et al., 2014), or due to less effective partitioning of semi-volatile organic compounds into aerosol particles at high temperatures during afternoon. Except of 28 August, the sky was cloud-free during our study period. Compared with the whole August−September period, the diurnal cycles of suphate and organic material during our case study period (Fig. 7b) were similar, even though less pronounced.

The diurnal variability in the aerosol chemical composition was reflected in the hygroscopic properties of particles at sizes critical to the cloud droplet activation (<150 nm). In Fig.8a the daily variation of the hygroscopicity (κ parameter) of 60−120 nm particles averaged over two full days is presented and in Fig. 8b the corresponding normalized values to the average κ of each diameter. As we may see, κ tended to decrease quite rapidly during early morning hours in our case study period, presumably due to the production of SOA of relatively low hygroscopicity. At some point around noon, the hygroscopicity of 80−120 nm particles started to increase again, as one would expect due to the formation of particulate sulphate at this time of the day. Smaller particles were much less hygroscopic than larger ones, the difference being 0.2−0.4 κ units between the 60 and 120 nm particles. A similar decrease in the value of κ when going below 100 nm in particle diameter has been reported in a few other field studies (Dusek et al., 2010; Cerully et al., 2011; Levin et al., 2012; Paramonov et al., 2013; Liu et al., 2014). This feature has been ascribed to the enrichment of organic material in sub-100 nm particles, combined with the usually more aged character of accumulation mode particles compared with sub-100 nm particles. Unfortunately, we had no size-resolved chemical aerosol measurements in our study period to look into this issue in more detail.

In addition to the relative amounts of sulfate to organic material, the character of the organic material influences aerosol hygroscopic properties (e.g. Chang et al., 2010; Moore et al., 2012; Kuwata et al., 2013; Cerully et al., 2014) although the link is tenuous or highly variable. By making a PMF analysis for the organic material measured by the ACSM, we found three major contributing factors: the factor OOA representing oxygenated organic aerosol, the factor OOA-BB that can be classified as processed biomass-burning organic aerosol, and the factor that resembles the SOA from α-pinene oxidation. Representative mass spectra of the first two of these factors can be found in Bougiatioti et al. (2014) and of the last one in Bahreini et al. (2005). During our case study period (Fig. 9), OOA explained the largest fraction of the total organic mass (average 46%), followed by OOA-BB (38%) and α-pinene SOA (16%). The high fraction of OOA-BB can be ascribed to the measured air masses being affected by forest fires in Croatia (Bougiatioti et al., 2014). The OOA observed at Finokalia during summer have multiple possible sources, including also aged biomass burning aerosol (Hildebrandt et al., 2010; Bougiatioti et al., 2014). The α-pinene SOA, while evident during our case study period when active NPF and growth was taking place, did not stand out during the rest of August−September, 2012. The O/C ratio of the organic material was close to or above unity during our case study period (Fig. 9), indicating that most of the organic compounds in aerosol particles were highly oxidized (see, e.g. Chang et al., 2010; Kuwata et al., 2013). The highest values of O/C were observed in the afternoon when the photochemical activity is at its highest, consistent with earlier findings at Finokalia (Hildebrandt et al., 2010). Since the SOA originating from the oxidation of α-pinene and many other terpenes is only slightly hygroscopic (e.g. Duplissy et al. 2008, Engelhart et al., 2011; Alfarra et al., 2013), its abundance before noon very likely contributed to the low κ values observed during that time of the day.

Finally, we investigated the mixing state of particles at sizes critical to CCN activation. The maximum values of AF remained above 0.8 for 80−120 nm particles, indicating that particles in this size range did not show a high degree of external mixture during our case study period (Fig. 10). Contrary to this, the maximum value of AF for 60 nm particles decreased substantially on 29 and 30 August (Fig. 10a). Interestingly, this decrease started approximately at the time when particles nucleated in the previous day had reached 60 nm as a result of their growth as can be seen in Fig. 10b that the average diurnal cycle of AF for these two days is presented. It therefore seems that there were two types of 60 nm particles during our case study period: those formed by recent atmospheric nucleation (less hygroscopic) and those that were more aged (more hygroscopic) ones. The origin of the latter particle type, whether nucleation or primary emissions,

remains unsolved. A similar observation has been reported for 40 nm particles by Cerully et al., (2011) in a boreal forest, attributing the low AF to not reaching the asymptote of the sigmoidal curve at the highest supersaturation measured for 40 nm spectra. The AF for 40 nm particles did not reach nevertheless as low AF as the ones shown in Fig.10 for 60 nm particles.

3.3 Implications for cloud droplet activation

Fig. 11 summarizes the cloud activating properties of 60, 80, 100 and 120 nm diameter particles during 29−30 August, 2012, the two days with a pronounced new particle formation and growth in our case study period. There are several things to be noted. First, the supersaturation required for cloud droplet activation increased more steeply with decreasing particle size than it would do if all the particles were equally hygroscopic. A similar feature has been observed in a few earlier studies (Levin et al., 2012; Paramonov et al., 2013; Liu et al., 2014), and it has generally been ascribed to the enrichment of organic material in ultrafine (<100 nm) particles. The main implication of this finding is that ultrafine particles tend to need higher cloud supersaturations to be able to act as CCN than one would expect based on the bulk chemical composition of the submicron particulate matter. Second, the hygroscopicity of 60−120 nm particles showed a clear diurnal cycle, with the minimum and maximum values of κ typically observed just before and after noon, respectively (Fig. 8). As discussed earlier, this feature was very likely due to higher sulfate to organic ratios (Fig. 7) and higher degree of oxidation of the organic material (Fig. 9) after noon. Fig. 7b suggests that the notable diurnal variability in the efficiency by which different-size particles act as CCN may be a common feature at Finokalia during summer. Finally, the required supersaturation needed for CCN activation varied easily by more than a factor 2 for given particle size even at the same time of the day, while the corresponding variability in the smallest diameter of particles able to act CCN at given cloud supersaturation was 20−30 nm.

The maximum supersaturation remains usually below 0.3% in polluted boundary layer clouds, while higher supersaturations close to or even larger than 1% have been reported under clean conditions and in convective clouds (Ditas et al., 2012; Hammer et al., 2014; Hudson and Noble, 2014). As discussed in Sect. 3.1, we were able to follow the growth of nucleated particles up to 50−60 nm in air masses measured in Finokalia during our case study period. Such particles would probably contribute little to the population of cloud droplets around Finokalia. However, we also found that the nuclei growth very likely continued to larger sizes, but at this point nucleated particles could not be separated from aged primary particles with the available measurements. We

conclude that aerosol nucleation taking place in the Eastern Mediterranean environment is capable of producing new CCN at cloud supersaturations encountered in this environment.

4. Conclusions

Atmospheric new particle formation (NPF) is a common phenomenon over the Eastern Mediterranean atmosphere, the observed frequency of NPF event days being close to 30% at Finokalia in Crete. However, there is practically no information whether particles formed in this environment are capable of producing new CCN and how effective this pathway is. The case study presented in this paper provides, for the first time, direct evidence on CCN production associated with atmospheric NPF and growth in the Eastern Mediterranean atmosphere. We found that, simultaneous with the formation of new particles during daytime, particles formed in the previous day or even earlier were growing into the size range relevant to cloud droplet activation, and that particles formed originally in the atmosphere were possibly mixed with long-range transported primary particles in the measured air masses. The complicated connection between primary and secondary CCN suggests it will be very difficult to close the regional CCN budget in terms of the most important CCN sources in this environment.

Aerosol chemical measurements suggest that both gaseous sulfuric acid and organic compounds play important roles in growing nucleated particles to CCN sizes over the Eastern Mediterranean during summertime. The organic compounds contributing to the nuclei growth appear to have multiple sources at this time of the year, including biogenic emissions, biomass burning and possibly other anthropogenic sources of distant origin. The hygroscopicity of particles critical to the cloud droplet activation (<150 nm diameter) were found to vary with both particle size and time of day. Small particles were substantially less hygroscopic than larger ones, probably due to enrichment of organic material in the sub-100 nm particles. Particles larger than 100 nm in diameter may be used as a proxy for CCN in the area. The aerosol hygroscopicity tended to be at minimum just before the noon and at maximum at some time in afternoon, which was very likely due to the higher sulfate to organic ratios and higher degree of oxidation of the organic material during afternoon. The diversity in the hygroscopic properties of sub-150 nm particles is clearly an issue requiring further attention.

This case study has demonstrated the power of simultaneous particle number size distribution, CCN and aerosols chemical measurements in investigating the origin of CCN in a polluted

marine environment, as well as their limitations in distinguishing sources and sinks. Understanding and quantification of the contribution of NPF to the CCN budget over Eastern Mediterranean would require comprehensive observations at extended time periods in this environment complemented with regional-scale aerosol dynamical model simulations.. Such measurements should include not only those applied here but also near-real time measurements of the size-resolved chemical composition of ultrafine (<100 nm) particles, gas-phase compounds responsible for the nuclei growth (sulphuric acid and extremely low-volatile organic compounds(see Ehn et al., 2014), potential precursors for low-volatile vapours (e.g. terpenes and organic compounds associated with biomass burning, see Vakkari et al., 2014), as well as the concentrations and size distributions of small (<3−10 nm) neutral and charged clusters. Interpretation of such measurements would benefit from some information on the diurnal evolution of the atmospheric boundary layer, volatility distributions as well as from both regional and smaller-scale modeling of aerosol-trace gas interactions in this environment.

5. Acknowledgements

The research project is implemented within the framework of the Action «Supporting Postdoctoral Researchers» of the Operational Program "Education and Lifelong Learning" (Action's Beneficiary: General Secretariat for Research and Technology), and is co-financed by the European Social Fund (ESF) and the Greek State. This research is supported by the Academy of Finland Center of Excellence program (project number 1118615). We acknowledge funding from the EU FP7-ENV-2013 program "impact of Biogenic vs. Anthropogenic emissions on Clouds and Climate: towards a Holistic UnderStanding" (BACCHUS), project no. 603445 The authors would like to acknowledge the NOAA Air Resources Laboratory (ARL) for the provision of the back trajectory data (http://www.arl.noaa.gov/ready/hysplit4.html). A. Nenes acknowledges support from an NSF CAREER proposal, NASA Lagley and NOAAOGP funding.

6. References

Aiken, A. C., DeCarlo, P. F., Kroll, J. H., Worsnop, D. R., Huffman, J. A., Docherty, K. S.,Ulbrich, I. M., Mohr, C., Kimmel,J. R., Sueper, D., Sun, Y., Zhang, Q., Trimborn, A., Northway,M., Ziemann, P., Canagaratna, M. R., Onasch, T. B., AlfarraM. R., Prévôt, A. H., Dommen, J., Duplissy, J., Metzger, A. Baltensperger, U., and Jimenez, J. L.: O/C and OM/OC

ratios of primary, secondary, and ambient organic aerosols with High-Resolution Time-of-Flight Aerosol Mass Spectrometry, Environ.Sci. Technol., 42, 4478–4485, doi:10.1021/es703009q, 2008.

Alfarra, M. R., Good, N., Wyche, K. P., Hamilton, J. F., Monks, P. S., Lewis, A. C., and McFiggans, G.: Water uptake is independent of the inferred composition of secondary aerosols derived from multiple biogenic VOCs, Atmos. Chem. Phys., 13, 11769−11789, doi:10.5194/acp-13-11769-2013, 2013.

Andreae, M. O. and Rosenfeld, D.: Aerosol–cloud–precipitation interactions. Part 1. The nature and sources of cloud-active aerosols, Earth-Science Reviews, 89, 13−41, doi:10.1016/j.earscirev.2008.03.001, 2008.

Bahreini, R., Keywood, M. D., Ng, N. L., Varutbangkul, V., Gao, S., Flagan, R., Seinfeld, J., Worsnop, D. R., and Jimenez, J. L.: Measurements of Secondary Organic Aerosol (SOA) from oxidation of cycloalkenes, terpenes, and m-xylene using an Aerodyne Aerosol Mass Spectrometer, Environ. Sci. Technol., 39, 5674–5688, doi:10.1021/es048061a, 2005.

Bardouki, H., Berresheim, H., Vrekoussis, M., Sciare, J., Kouvarakis, G., Oikonomou, K., Schneider, J., and Mihalopoulos, N: Gaseous (DMS, MSA, SO_2, H_2SO_4, and DMSO) and particulate (sulfate and methanesulfonate) sulfur species over the northeastern coast of Crete, Atmos. Chem. Phys., 3, 1871–1886, doi:10.5194/acp-3-1871-2003, 2003.

Bougiatioti, A., Fountoukis, C., Kalivitis, N., Pandis, S. N., Nenes, A., and Mihalopoulos, N.: Cloud condensation nuclei measurements in the marine boundary layer of the eastern Mediterranean: CCN closure and droplet growth kinetics, Atmos. Chem. Phys., 9, 7053–7066, doi:10.5194/acp-9-7053-2009, 2009.

Bougiatioti, A., Nenes, A., Fountoukis, C., Kalivitis, N., Pandis, S. N., and Mihalopoulos, N.: Size-resolved CCN distributions and activation kinetics of aged continental and marine aerosol, Atmos. Chem. Phys., 11, 8791–8808, doi:10.5194/acp-11-8791-2011, 2011.

Bougiatioti, A., Zarmpas, P., Koulouri, E., Antonou, M., Theodosi, C., Kouvarakis, G., Saarikoski, S., Mäkelä, T., Hillamo, R., and Mihalopoulos, N.: Organic, elemental and water-soluble organic carbon in size segregated aerosols, in the marine boundary layer of the Eastern Medeterranean, Atmos. Environ., 64, 251−252, doi:10.1016/j.atmosenv.2012.09.071, 2013.

Bougiatioti, A., Stavroulas, I., Kostenidou, E., Zarmpas, P., Theodosi, C., Kouvarakis, G.,Canonaco, F., Prévôt, A. S. H., Nenes, A.,Pandis, S. N., and Mihalopoulos, N.: Processing of biomass-burning aerosol in the eastern Mediterranean during summertime, Atmos. Chem. Phys., 14, 4793−4807, doi:10.5194/acp-14-4793-2041, 2014.

Canonaco, F., Crippa, M., Slowik, J. G., Prévôt, A. S. H., and Baltensperger, U.: SoFi, an Igor based interface for the efficient use of the generalized multilinear engine (ME-2) for source apportionment: application to aerosol mass spectrometer data, Atmos. Meas. Tech. Discuss., 6,6409 - 6443, doi: 10.5194/amtd-6-6409-2013, 2013.

Cerully K.M., Raatikainen T., Lance S., Tkacik D., Tiitta, P., Petäjä T., Ehn M., Kulmala M., Worsnop D.R., Laaksonen A., Smith J.N., and Nenes A.: Aerosol hygroscopicity and CCN activation kinetics in a boreal forest environment during the 2007 EUCAARI campaign, Atmos. Chem. Phys.11: 12369–12386, doi:10.5194/acp-11-12369-2011, 2011.

Cerully, K. M., Bougiatioti, A., Hite Jr., J. R., Guo, H., Xu, L., Ng, N. L., Weber, R., and Nenes, A.: On the link between hygroscopicity, volatility, and oxidation state of ambient and water-soluble aerosol in the Southeastern United States, Atmos. Chem. Phys. Discuss., 14, 30835-30877, doi:10.5194/acpd-14-30835-2014, 2014.Chang, R. Y-W., Slowik, J. G., Shantz, N. C., Vlasenko, A., Liggio, J.,Sjostedt, S. J., Leaitch, W. R., and Abbatt, J. P. D.: The hygroscopicity parameter (κ) of ambient organic aerosol at a field site subject to biogenic and anthropogenic influences: relationship to degree of aerosol oxidation, Atmos. Chem. Phys., 10, 5047−5064, doi:10.5194/acp-10-5047-2010, 2010.

Ditas, F., Shaw, R. A., Siebert, H., Simmel, M., Wehner, B., and Wiedensohler, A.: Aerosol-cloud microphysics-thermodynamics-turbulence: evaluating supersaturation in a marine stratocumulus cloud, Atmos. Chem. Phys., 12, doi:10.5194/acp-12-2459-2012, 2012.

Dowd, C. D. O.: Biogenic coastal aerosol production and its influence on aerosol radiative properties, J. Geophys. Res., 106(D2), 1545–1549, doi:10.1029/2000JD900423, 2001.

Draxler, R. R., and Hess, G. D.: An overview of the HYSPLIT 4 modeling system of trajectories, dispersion, and deposition, Aust. Meteor. Mag., 47, 295−308, 1998.

Duplissy, J., Gysel, M., Alfarra, M. R., Dommen, J., Metzger, A., Prevot, A. S. H., Weingartner, E., Laaksonen, A., Raatikainen, T., Good, N., Turner, S. F., McFiggans, G., and Baltensperger,

U.: Cloud forming potential of secondary organic aerosol under near atmospheric conditions, Geophys. Res. Lett., 35, L03818, doi:10.1029/2007GL031075, 2008..

Dusek, U., Frank, G. P., Hildebrandt, L., Curtius, J., Schneider, J.., Walter, S., Chand, D., Drewnick, F., Hings, S., Jung, D., Borrmann, S., and Andreae, M. O.: Size matters more than chemistry for cloud-nucleating ability of aerosol particles, Science, 312, 1375−1378, doi: Science, 312, 1375−1378, 2006.

Dusek,U.,Frank, G. P., Curtius, J., Drewnick, F., Schneider, J., Kürten, A., Rose, D., Andreae, M. O., Borrmann, S., and Pöschl, U.: Enhanced organic mass fraction and decreased hygroscopicity of cloud condensation nuclei (CCN) during NPF events, Geophys. Res. Lett., 37, L03804, doi:10.1029/2009GL040930, 2010.

Ehn, M., Thornton, J. A., Kleist, E., Sipilä, M., Junninen, H., Pullinen, I., Springer, M., Rubach, F., Tillmann, R., Lee, B., Lopez-Hifiker, F., Andres, S., Acir, I.H., Rissanen, M., Jokinen, T., Schobesberger, S., Kangasluoma, J., Kontkanen, J., Nieminen, T., Kurten, T., Nielsen, L. B., Jorgensen, S., Jaergaard, H. G., Canagaratna, M., Dal Maso, M., Berndt, T., Petäjä, T., Wahner,A., Kerminen, V.-M., Kulmala, M., Worsnop, D., Wildt, J., and Mentel, T. F.: A large source of low-volatility secondary organic aerosol, Nature, 506, 476−479, doi:10.1038/nature13032, 2014.

Engelhart, G. J., Moore, R. H., Nenes, A., and Pandis, S. N.: Cloud condensation nuclei activity of isoprene secondary organic aerosol, J. Geophys. Res., 116, D02207, doi:10.1029/2010JD014706, 2011.

Hammer, E., Bukowiecki, N., Gysel, M., Juranyi, Z., Hoyle, C. R., Vogt, R., Baltensperger, U., and Weingartner, E.: Investigation of the effective peak supersaturation for liquid-phase clouds at the high-alpine site Jungfraujoch, Switzerland, Atmos. Chem. Phys., 14, 1123−1139, doi:10.5194/acp-14-1123-2014, 2014.

Hildebrandt, L., Engelhart, G. J., Mohr, C., Kostenidou, E., Lanz, V. A., Bougiatioti, A., DeCarlo, P. F., Prevot, A. S. H., Baltensperger, U., Mihalopoulos, N., Donahue, N. M., and Pandis, S. N.: Aged organic aerosol in the Eastern Mediterranean: the Finokalia Aerosol Measurement Experiment – 2008, Atmos. Chem. Phys., 10, 4167-4186, doi:10.5194/acp-10-4167-2010, 2010.

Hudson, J. G. and Noble, S.: CCN and vertical velocity influences on droplet concentrations and supersaturations in clean and polluted stratus clouds, J. Atmos. Sci., 71, 312−331, doi: 10.1175/JAS-D-13-086.1, 2014.

IPCC, 2013: Climate Change 2013: The Physical Science Basis. Contribution of Working Group I to the Fifth Assessment Report of the Intergovernmental Panel on Climate Change [Stocker, T.F., D. Qin, G.-K. Plattner, M. Tignor, S.K. Allen, J. Boschung, A. Nauels, Y. Xia, V. Bex and P.M. Midgley (eds.)]. Cambridge University Press, Cambridge, United Kingdom and New York, NY, USA, 1535 pp, doi:10.1017/CBO9781107415324, 2013 Kalivitis, N., Birmili, W., Stock, M., Wehner, B., Massling, A., Wiedensohler, A., Gerasopoulos, E., and Mihalopoulos, N.: Particle size distributions in the Eastern Mediterranean troposphere, Atmos. Chem. Phys., 8, 6729–6738, doi:10.5194/acp-8-6729-2008, 2008.

Kalivitis, N., Stavroulas, I., Bougiatioti, A., Kouvarakis, G., Gagné, S., Manninen, H. E., Kulmala, M., and Mihalopoulos, N.: Night-time enhanced atmospheric ion concentrations in the marine boundary layer, Atmos. Chem. Phys., 12, 3627−3638, doi:10.5194/acp-12-3627-2012, 2012.

Karydis, V. A., Capps, S. L., Russell, A. G., and Nenes, A.: Adjoint sensitivity of global cloud droplet number to aerosol and dynamical parameters, Atmos. Chem. Phys., 12, 9041-9055, doi:10.5194/acp-12-9041-2012, 2012. Kerminen, V.-M., Paramonov, M., Anttila, T., Riipinen, I., Fountoukis, C., Korhonen, H., Asmi, E., Laakso, L., Lihavainen, H., Swietlicki, E., Svenningsson, B., Asmi, A., Pandis, S. N., Kulmala, M., and Petäjä, T.: Cloud condensation nuclei production associated with atmospheric nucleation: a synthesis based on existing literature and new results, Atmos. Chem. Phys., 12, 12037–12059, doi:10.5194/acp-12-12037-2012, 2012.

Kouvarakis, G. and Mihalopoulos, N.: Seasonal variation of dimethylsulfide in the gas phase and of methanesulfonate and non-sea-salt sulfate in the aerosols phase in the Eastern Mediterranean atmosphere, Atmos. Environ., 36, 929−938, doi: 10.1016/S1352-2310(01)00511-8, 2002.

Kulmala, M., Petäjä, T., Nieminen, T., Sipilä, M., Manninen, H.E., Lehtipalo, K., Dal Maso, M., Aalto, P. P., Junninen, H., Paasonen, P., Riipinen, I., Lehtinen, K. E. J., Laaksonen, A., andKerminen, V.-M.: Measurement of the nucleation of atmospheric aerosol particles, Nat. Protoc., 7, 1651–1667, doi:10.1038/nprot.2012.091, 2012.

Kuwata, M., Shao, W., Lebouteiller, R., and Martin, S. T.: Classifying organic materials by oxygen-to-carbon elemental ratio to predict the activation regime of Cloud Condensation Nuclei (CCN), Atmos. Chem. Phys., 13, 5309−5324, doi:10.5194/acp-13-5309-2013, 2013.

Laakso, L., Merikanto, J., Vakkari, V., Laakso, H., Kulmala, M., Molefe, M., Kgabi, N., Mabaso, D., Carslaw, K. S., Spracklen, D. V., Lee, L. A., Reddington, C. L., and Kerminen, V.-M.: Boundary layer nucleation as a source of new CCN in savannah environment, Atmos. Chem. Phys., 13, 1957–1972, doi:10.5194/acp-13-1957-2013, 2013.

Lelieveld, J., Berresheim, H., Borrmann, S., Crutzen, P., Dentener, F., Fischer, H., Feichter, J., Flatau, P., Heland, J., Holzinger, R., Korrmann, R., Lawrence, M., Levin, Z., Markowicz, K., Mihalopoulos, N., Minikin, A., Ramanathan, V., de Reus, M., Roelofs, G., Scheeren, H., Sciare, J., Schlager, H., Schultz, M., Siegmund, P., Steil, B., Stephanou, E., Stier, P., Traub, M., Warneke, C., Williams, J., and Ziereis, H.: Global air pollution crossroads over the Mediterranean, Science, 298, 794–799, doi: 10.1126/science.1075457, 2002.

Levin, E. J. T., Prenni, A. J., Petters, M. D., Kreidenweis, S. M., Sullivan, R. C., Atwood, S. A., Ortega, J., DeMott, P. J., and Smith, J. N.: An annual cycle of size-resolved aerosol hygroscopicity at a forested site in Colorado, J. Geophys. Res., 117, D06201, doi:10.1029/2011JD016854, 2012.

Liu, H. J., Zhao, C. S., Nekat, B., Ma, N., Wiedensohler, A., van Pinxteren, D., Spindler, G., Müller, K., and Herrmann, H.: Aerosol hygroscopicity derived from size-segregated chemical composition and its parameterization in the North China Plain, Atmos. Chem. Phys., 14, 2525−2539, doi:10.5194/acp-14-2525-2014, 2014.

Manninen, H. E., Nieminen, T., Asmi, E., Gagné, S., Hàakkinen, S., Lehtipalo, K., Aalto, P., Vana, M., Mirme, A., Mirme, S., Hõrrak, U., Plass-Dülmer, C., Stange, G., Kiss, G., Hoffer, A., Törõ, N., Moerman, M., Henzing, B., de Leeuw, G., Brinkenberg, M., Kouvarakis, G. N., Bougiatioti, A., Mihalopoulos, N., O'Dowd, C., Ceburnis, D., Arneth, A., Svenningsson, B., Swietlicki, E., Tarozzi, L., Decesari, S., Facchini, M. C., Birmili, W., Sonntag, A., Wiedensohler, A., Boulon, J., Sellegri, K., Laj, P., Gysel, M., Bukowiecki, N., Weingartner, E., Wehrle, G., Laaksonen, A., Hamed, A., Joutsensaari, J., Petäjä, T., Kerminen, V.-M., and Kulmala, M.: EUCAARI ion spectrometer measurements at 12 European sites – analysis of NPF events, Atmos. Chem. Phys., 10, 7907–7927, doi:10.5194/acp-10-7907-2010, 2010.

Massoli, P., Lambe, A. T., Ahern, A. T., Williams, L. R., Ehn, M., Mikkilä, J., Canagaratna, M. R., Brune, W. H., Onasch, T. B., Jayne, J. T., Petäjä, T., Kulmala, M., Laaksonen, A., Kolb, C. E., Davidovits, P., and Worsnop, D. R.: Relationship between aerosol oxidation level and hygroscopic properties of laboratory generated secondary organic aerosol (SOA) particles, Geophys. Res. Lett., 37, L24801, doi:10.1029/2010GL045258, 2010.

Mei, F., Hayes, P. L., Ortega, A., Taylor, J. W., Allan, J. D., Gilman, J., Kuster, W., de Gouw, J., Jimenez, J. L., and Wang, J.: Droplet activation properties of organic aerosols observed at an urban site during CalNex-LA, J. Geophys. Res. Atmos., 118, 2903–2917, doi:10.1002/jgrd.50285, 2013.

Merikanto, J., Spracklen, D. V., Mann, G. W., Pickering, S. J., and Carslaw, K. S.: Impact of nucleation on global CCN, Atmos. Chem. Phys., 9, 8601−8616, doi:10.5194/acp-9-8601-2009, 2009.

Mihalopoulos, N., Stephanou, E., Kanakidou, M., Pilitsidis, S., and Bousquet, P.: Tropospheric aerosol ionic composition in the Eastern Mediterranean region, Tellus Series B - Chemical and Physical Meteorology, 49, 314– 326, 1997.

Mihalopoulos, N., Kerminen, V.-M., Kanakidou, M., Berresheim, H., and Sciare, J.: Formation of particulate sulphur species (sulphate and methanesulfonate) during summer over the Eastern Mediterranean: A modelling approach, Atmos. Environ., 41, 6860-6871, doi:10.1016/j.atmosenv.2007.04.039, 2007.

Moore, R. H. and Nenes, A.: Scanning Flow CCN Analysis - A Method for Fast Measurements of CCN Spectra, Aerosol Sci. Tech., 43, 1192−1207, doi:10.1080/02786820903289780, 2009.

Moore, R.H., Cerully, K., Bahreini, R., Brock, C.A., Middelbrook, A.M., and Nenes, A.: Hygroscopicity and composition of California CCN during summer 2010, J. Geophys. Res., 117, D00V12, doi:10.1029/2011JD017352, 2012.

Ng, N. L., Herndon, S. C., Trimborn, A., Canagaratna, M. R., Croteau, P. L., Onasch, T. B., Sueper, D., Worsnop, D. R., Zhang, Q., Sun, Y. L., and Jayne, J. T.: An Aerosol Chemical Speciation Monitor (ACSM) for routine monitoring of the composition and mass concentration of ambient aerosol., Aerosol Sci. Tech., 45, 780–794, doi:10.1080/02786826.2011.560211, 2011.

Paasonen, P., Asmi, A., Petäjä, T., Kajos, M. K., Aijala, M., Junninen, H., Holst, T.,Abbatt, J. P. D., Arneth, A., Birmili, W., van der Gon, H. D., Hamed, A., Hoer,A., Laakso, L., Laaksonen, A., Richard Leaitch, W., Plass-Dulmer, C., Pryor, S. C.,Raisanen, P., Swietlicki, E., Wiedensohler, A., Worsnop, D. R., Kerminen, V.-M.,and Kulmala, M.,: Warming-induced increase in aerosol number concentration likely to moderate climate change, Nature Geosci., 6(6):438-442, doi:10.1038/ngeo1800, 2013.

Paatero, P.: The multilinear engine - A table-driven, least squares program for solving multilinear problems, including the n-way parallel factor analysis model, J. Comp. Graph. Stat., 8, 854−888, doi:10.2307/1390831, 1999.

Paramonov M., P. P. Aalto, A. Asmi, N. Prisle, V.-M. Kerminen, M. Kulmala, and T. Petäjä, The analysis of size-segregated cloud condensation nuclei counter (CCNC) data and its implications for cloud droplet activation, Atmos. Chem. Phys., 13, 10285−10301, doi:10.5194/acp-13-10285-2013, 2013.

Padró, L. T., Moore, R. H., Zhang, X., Rastogi, N., Weber, R. J., and Nenes, A.: Mixing state and compositional effects on CCN activity and droplet growth kinetics of size-resolved CCN in an urban environment, Atmos. Chem. Phys., 12, 10239–10255, doi:10.5194/acp-12-10239-2012, 2012.

Petäjä, T., Kerminen, V.-M., Dal Maso, M., Junninen, H., Koponen, I.K., Hussein, T., Aalto, P.P., Andronopoulos, S., Robin, D., Hämeri, K., Bartzis, J.G. and Kulmala, M. Sub-micron atmospheric aerosols in the surroundings of Marseille and Athens: physical characterization and new particle formation. Atmos. Chem. Phys., 7, pp. 2705-2720, doi:10.5194/acp-7-2705-2007, 2007.

Petters, M. D. and Kreidenweis, S. M.: A single parameter representation of aerosol hygroscopicity and cloud condensation nucleus activity, Atmos. Chem. Phys., 7, 1961–1971, doi:10.5194/acp-7-1961-2007, 2007.

Pierce, J. R. and Adams, P. J.: Uncertainty in global CCN concentrations from uncertain aerosol nucleation and primary emission rates, Atmos. Chem. Phys., 9, 1339−1356, doi:10.5194/acp-9-1339-2009, 2009.

Pikridas, M., I. Riipinen, L. Hildebrandt, E. Kostenidou, H. Manninen, N. Mihalopoulos, N. Kalivitis, J. Burkhart, A. Stohl, M. Kulmala, S. N. Pandis, NPF at a remote site in the eastern Mediterranean, J. Geophys. Res., 117, D12205, doi:10.1029/2012JD017570, 2012.

Pruppacher, H. R. and Klett, J. D.: Microphysics of clouds and precipitation, Kluwer Academic Publishers, Dordrecht, The Netherlands, 1997.

Roberts, G., and Nenes, A.: A continuous-flow streamwise thermal-gradient CCN chamber for atmospheric measurements, Aerosol Sci. Technol., 39, 206–221, doi:10.1080/027868290913988, 2005.

Sciare, J., Oikonomou, K., Cachier, H., Mihalopoulos, N., Andreae, M.O., Maenhaut, W., and Sarda-Esteve, R.: Aerosol mass closure and reconstruction of the light scattering coefficient over the Eastern Mediterranean Sea during the MINOS campaign, Atmos. Chem. Phys. 5, 2253–2265, doi:10.5194/acp-5-2253-2005, 2005.

Vakkari, V., Kerminen, V.-M., Beukes, J. P., Tiitta, P., van Zyl, P. G., Josipovic, M., Venter, A. D., Jaars, K., Worsnop, D. R., Kulmala, M., and Laakso L.: Rapid changes in biomass burning aerosols by atmospheric oxidation, Geophys. Res. Lett., 41, 2644−2651, doi: 10.1002/2014GL059396, 2014.

Weingartner, E., Saathoff, H., Schnaiter, M., Streit, N., Bitnar, B., and Baltensperger, U.: Absorption of light by soot particles: determination of the absorption coefficient by means of aethalometers, J. Aerosol Sci., 34, 1445–1463, doi:10.1016/S0021-8502(03)00359-8, 2003.

Westervelt, D. M., Pierce, J. R., and Adams, P. J.: Analysis of feedbacks between nucleation rate, survival probability and cloud condensation nuclei formation, Atmos. Chem. Phys., 14, doi:10.5194/acp-14-5577-2014, 2014.

Wiedensohler, A., Birmili, W., Nowak, A., Sonntag, A., Weinhold, K., Merkel, M., Wehner, B., Tuch, T., Pfeifer, S., Fiebig, M., Fjäraa, A. M., Asmi, E., Sellegri, K., Depuy, R., Venzac, H., Villani, P., Laj, P., Aalto, P., Ogren, J. A., Swietlicki, E., Williams, P., Roldin, P., Quincey, P., Hüglin, C., Fierz-Schmidhauser, R., Gysel, M., Weingartner, E., Riccobono, F., Santos, S., Grüning, C., Faloon, K., Beddows, D., Harrison, R., Monahan, C., Jennings, S. G., O'Dowd, C. D., Marinoni, A., Horn, H.-G., Keck, L., Jiang, J., Scheckman, J., McMurry, P. H., Deng, Z.,

Zhao, C. S., Moerman, M., Henzing, B., de Leeuw, G., Löschau, G., and Bastian, S.: Mobility particle size spectrometers: harmonization of technical standards and data structure to facilitate high quality long-term observations of atmospheric particle number size distributions, Atmos. Meas. Tech., 5, 657-685, doi:10.5194/amt-5-657-2012, 2012.

Yu, F. and Luo, G.: Simulation of particle size distribution with a global aerosol model: contribution of nucleation to aerosol and CCN number concentrations, Atmos. Chem. Phys., 9, 7691–7710, doi:10.5194/acp-9-7691-2009, 2009

Zerefos, C., Ganev, K., Kourtidis, K., Tzortziou, M., Vasaras, A., and Syrakov,E.: On the origin of SO_2 above northern Greece, Geophysical Research Letters, 27,365-368, doi: 10.1029/1999GL010799, 2000

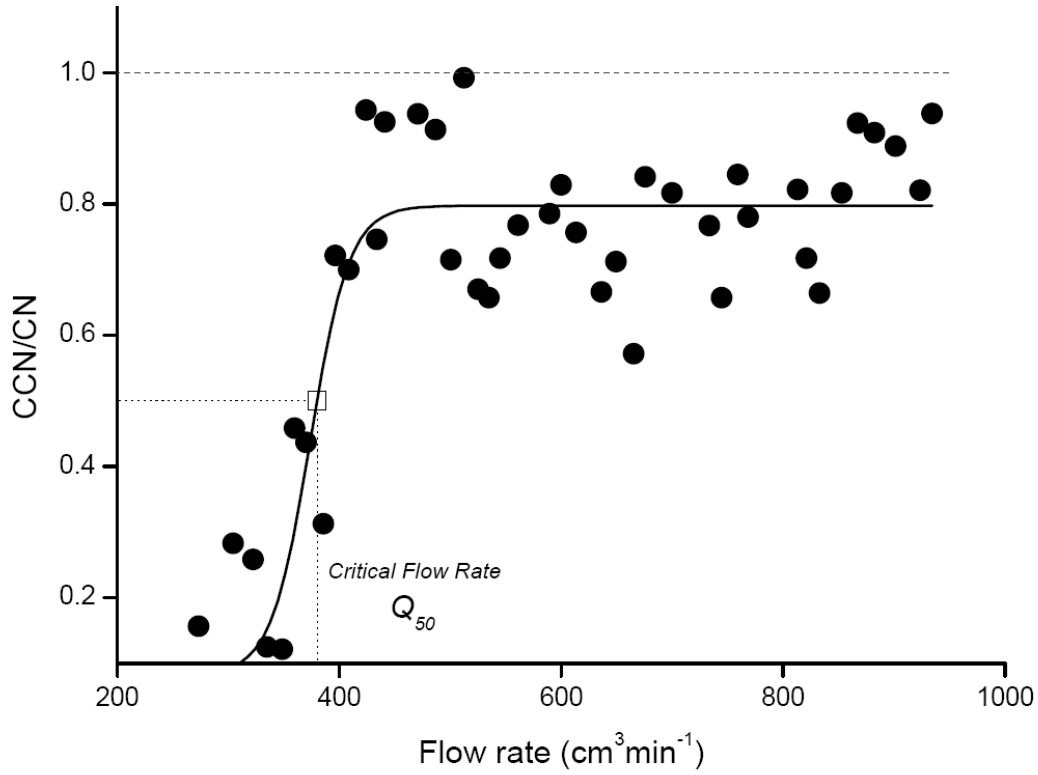

Fig1. Example of an ambient CCN activity spectrum (at a constant temperature difference), with a sigmoidal fit and the associated critical flow Q_{50}.

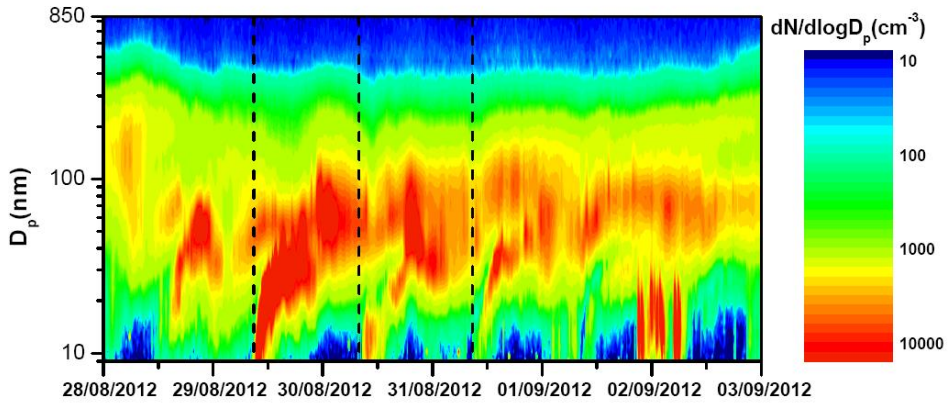

Fig. 2. Time evolution of the particle number size distribution over the diameter range 9–848 nm between 28 August and 2 September, 2012, a period of active new particle formation observed at Finokalia. The dashed vertical lines in the figure indicate the times when newly formed particles started to appear to the measured size spectra during the three NPF events concentrated in our analysis.

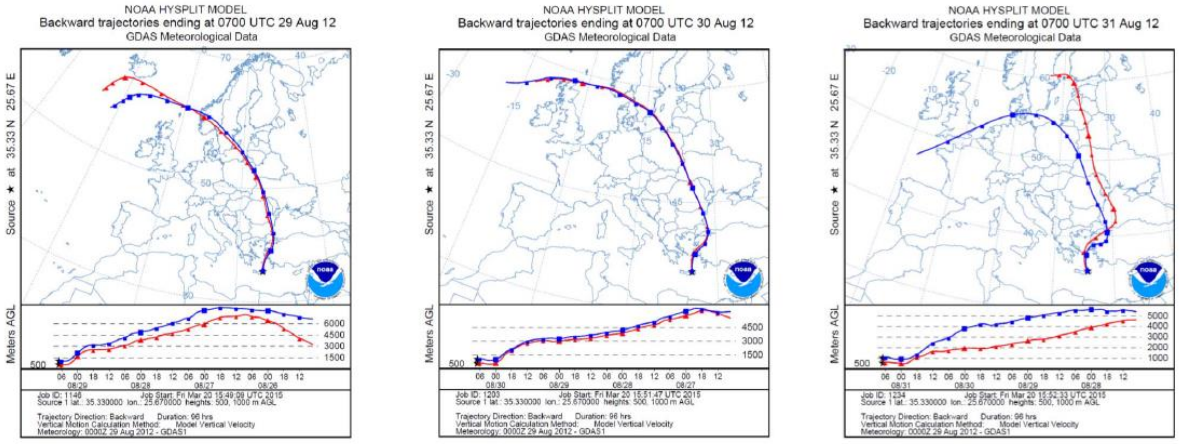

Fig. 3.Four-day back trajectories for air masses arriving at Finokalia on 29, 30 and 31 August, 2012.

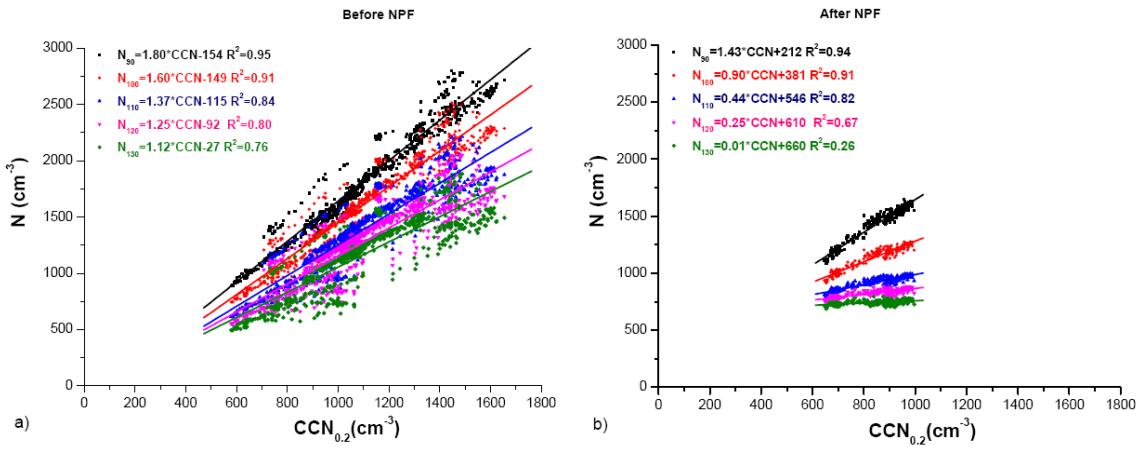

Fig. 4. Relation between the total number concentration of particles with diameter larger than D, N_D, (D = 90, 100, 110, 120 or 130 nm) and measured CCN number concentration at the supersaturation of 0.2 %. The data are from two periods in 2012: from 25 August at 23:05 to 28 August at 10:45 (panel a) and from 1 September at 23:15 to 2 September at 17:15 UTC+2 (panel b).

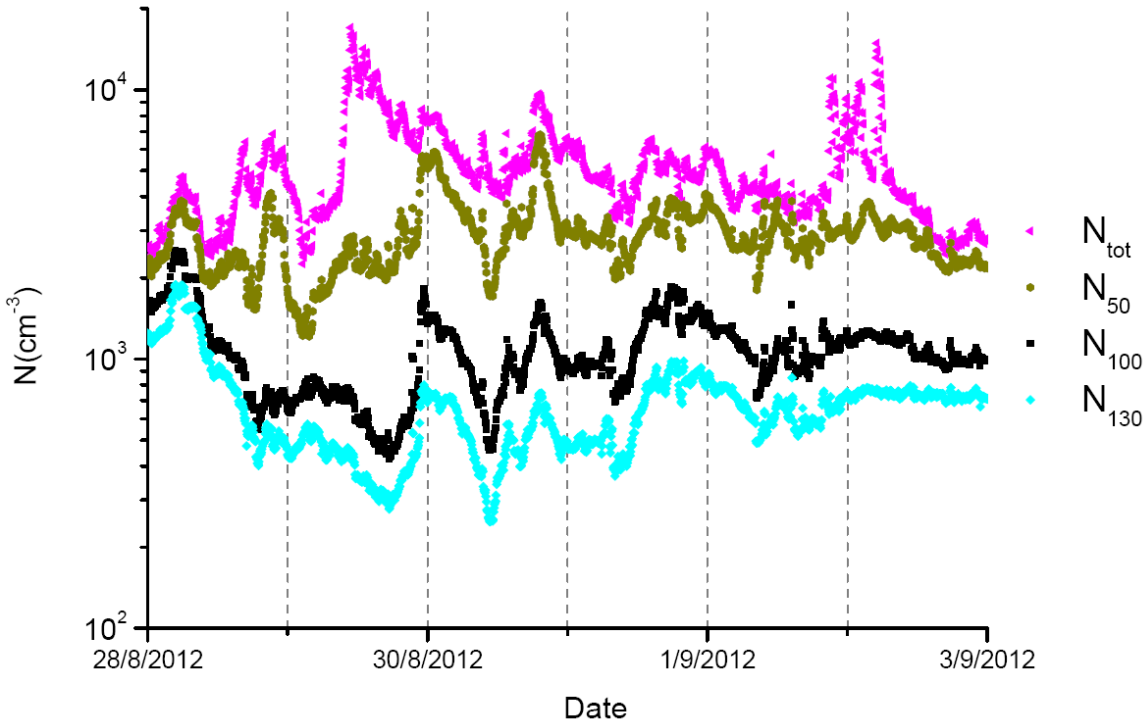

Fig. 5. Time evolution of the total particle number concentration (N_{tot}) along with N_{50}, N_{100} and N_{130} during the period 28 August – 2 September, 2012.

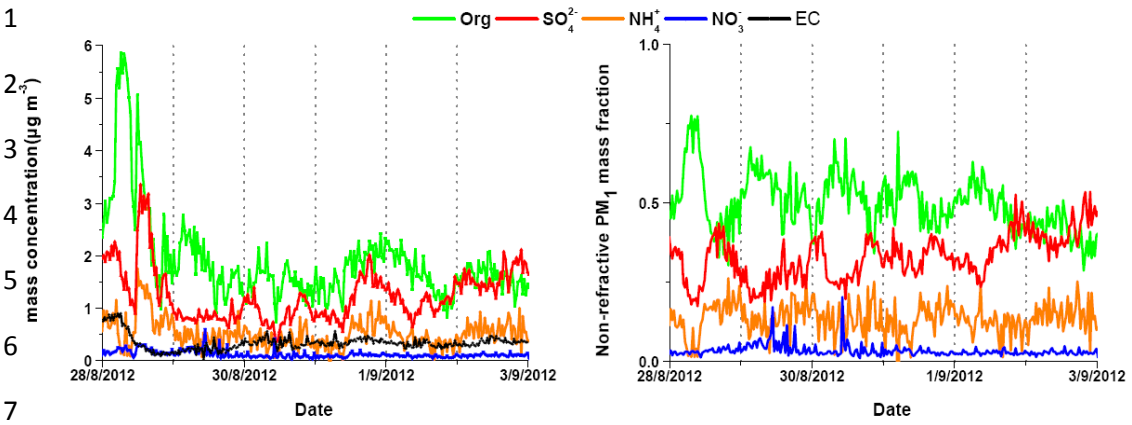

Fig. 6. Time evolution of the aerosol chemical composition during the period 28 August – 2 September 2012. Left panel: absolute concentrations (µg m^{-3}) in the PM_1 fraction of the measured aerosol, except for EC which was measured in the PM_{10} fraction. Right panel: relative contributions to the non-refractive PM_1 mass

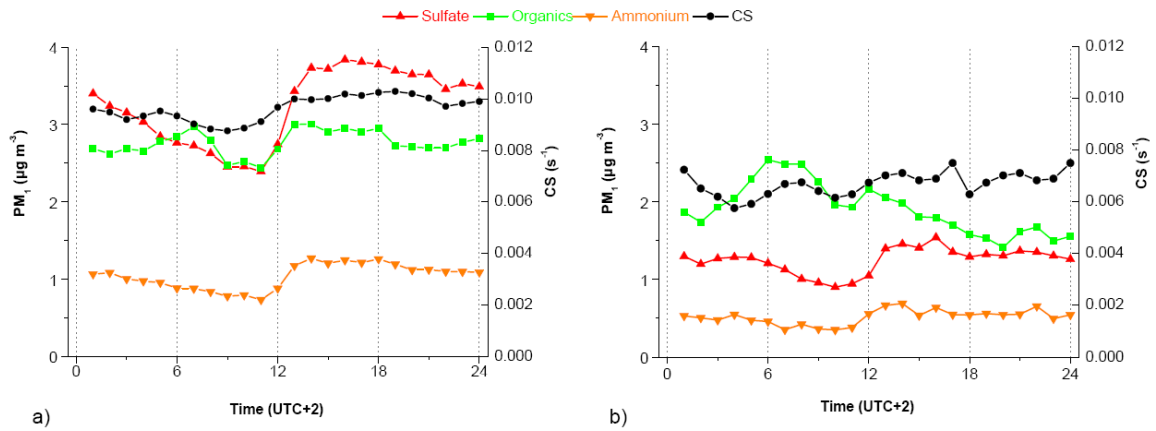

Fig. 7. Diurnal concentration cycles of sulfate, ammonium and organic material in sub-micron aerosols, as well as the diurnal cycle of condensation sink, CS, averaged over the 1 August-30 September period (a) and over the period 28 August – 2 September (b) in 2012.

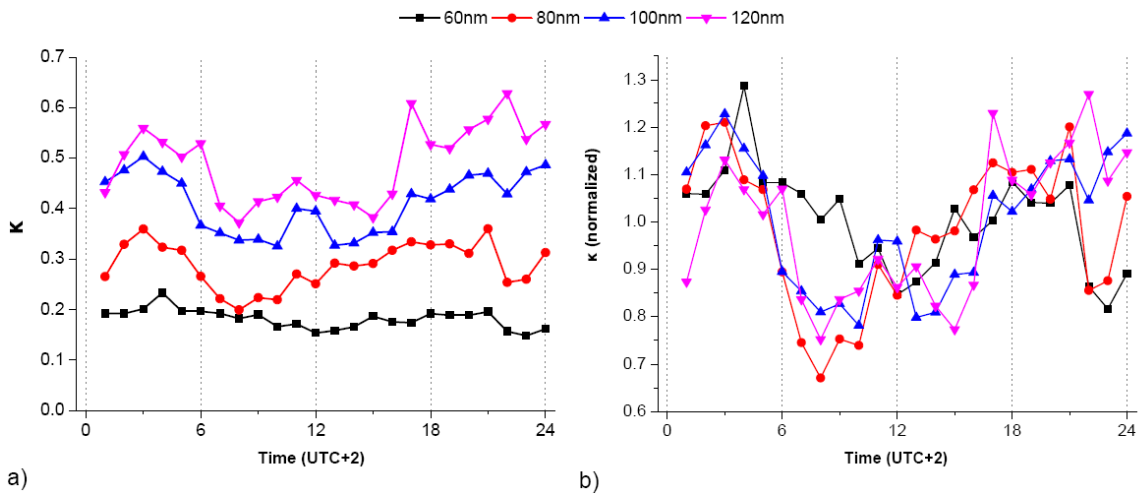

Fig. 8. Diurnal variability during the period from 28 August at 12:00 to 30 August at 12:00 of a) the hygrocopicity parameters κ for 60, 80, 100 and 120 nm particles and b) the corresponding values normalized to the average κ value for each diameter.

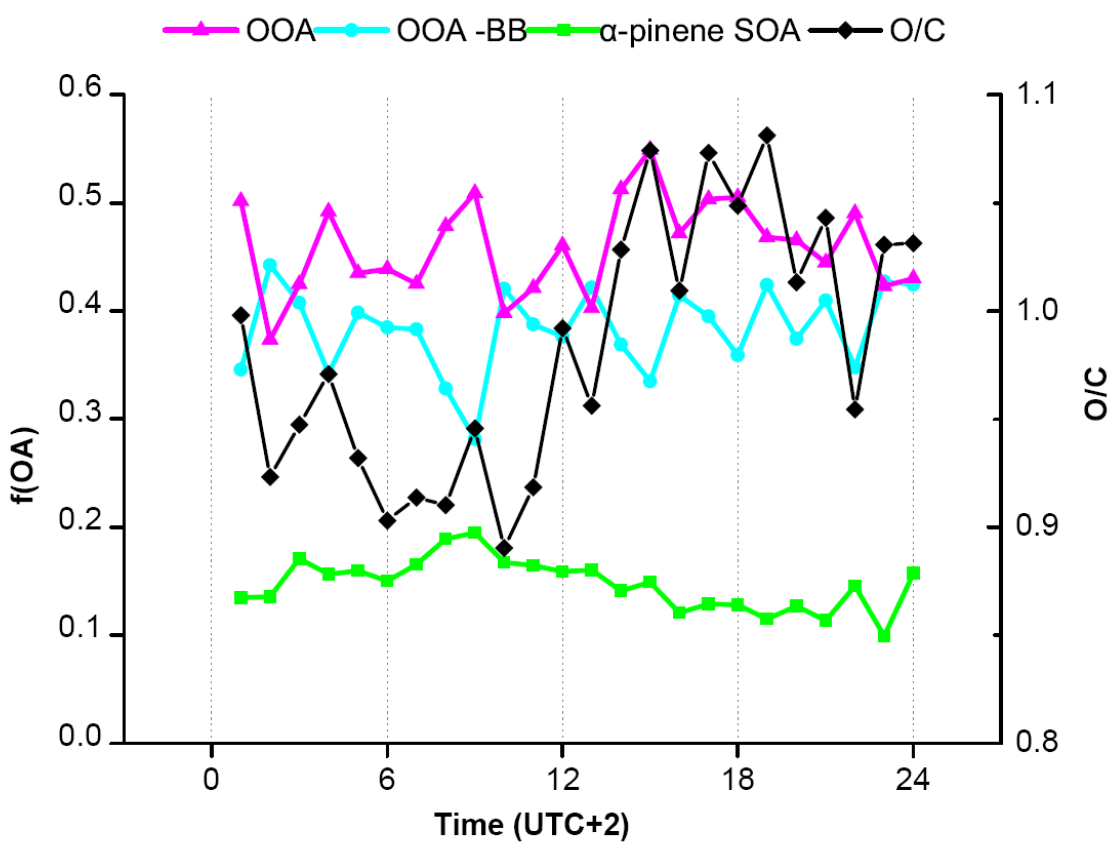

Fig. 9. Diurnal variability of the three major classes of organic aerosol obtained from the PMF analysis, along with the O/C ratio, during the period 28 August to 2 September. The quantity f(OA) represents the fractions of individual organic compounds of the total organic mass, where OA refers to OOA, OOA-BB or α-pinene SOA.

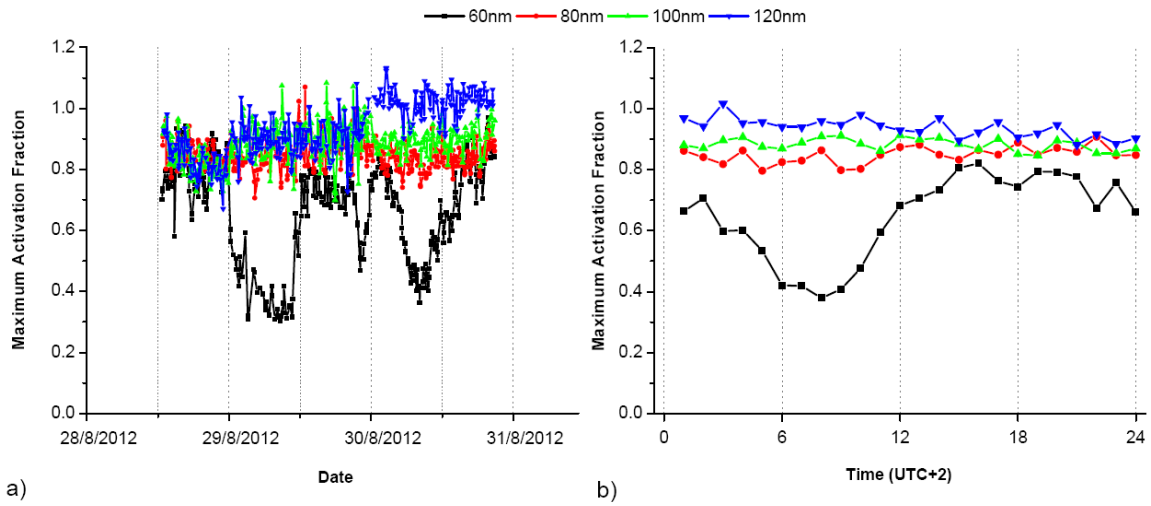

Fig. 10. a) Maximum activation fraction of 60,80, 100 and 120 nm particles between 28 and 30 August, 2012. b) Diurnal cycle of the maximum activated fraction for the same period.

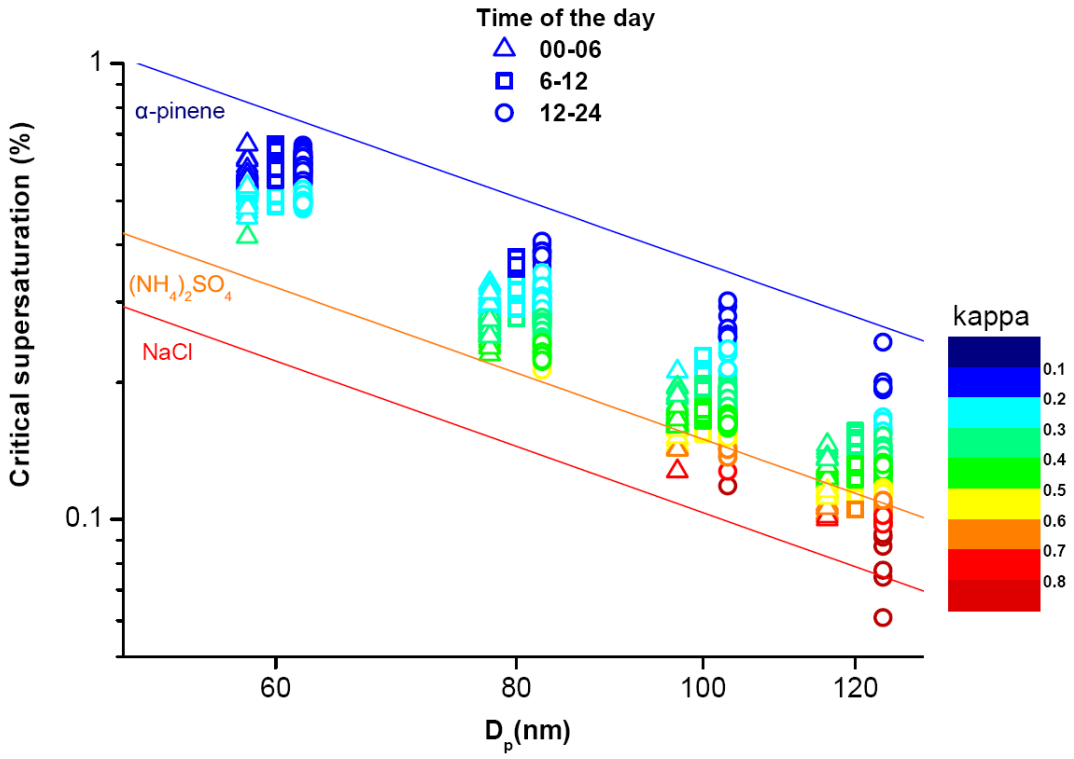

Fig. 11. Measured critical supersaturations of 60, 80, 100 and 120 nm diameter particles during different times of the day on 28 and 30 August, 2012. The color scale indicates different values of the particle hygroscopicity parameter, κ. Also, theoretical curves for α-pinene, ammonium sulfate and sodium chloride.